Hydrology Research

British Hydrological Society

IWA PUBLISHING

Hydrology Research Vol 52 No 6, 1615 doi: 10.2166/nh.2021.085

Quantitative accuracy assessment of the revised sparse Gash model using distinct time-step climatic parameters

Yiran Li[a,b], Chuanjie Zhang[c] and Yong Niu[a,*]

[a] College of Forestry, Shandong Agricultural University, Shandong 271018, China
[b] School of Soil and Water Conservation, Beijing Forestry University, Beijing 100083, China
[c] College of Water Conservancy and Civil Engineering, Shandong Agricultural University, Shandong 271018, China
*Corresponding author. E-mail: niuyong1988@126.com
Yiran Li and Chuanjie Zhang contributed equally to this work.

ABSTRACT

Rainfall interception (*I*) can considerably influence the transport process of water. The revised sparse Gash model (RSGM) is a tool for determining the *I*, which assumes that the two climate parameters in the model are equal for all storms. However, few studies have provided additional cases to reexamine the correctness of this assumption and investigated the response of *I* of single storms to the time-step variability in climatic parameters. Hence, rainfall partitioning was measured during the growing season in 2017 for *Pinus tabuliformis, Platycladus orientalis, and Acer truncatum* in Northern China, and we ran RSGM on an event basis using different time-step climatic parameters (storm-based, monthly, and fixed) to estimate *I*. In summary, the modeling accuracy of both cumulative *I* and individual *I* was enhanced by increasing the time step of the climatic parameters in this study. These positively support the assumption in the RSGM. These results suggest that it is more appropriate to run the RSGM using fixed climate parameters to estimate *I* for these tree species during the growing season in northern China. Additionally, the assumption in the RSGM should be appealed to be further confirmed across the widest possible range of species, regions, and time scales.

Key words: potential counteracting mechanism, rainfall interception, revised sparse Gash model, sensitivity analysis

HIGHLIGHTS

- The reasonableness of an assumption in the revised sparse Gash model (RSGM) was reexamined.
- Effects of time-step climatic parameters on the RSGM were compared.
- Fixed climatic parameters were more appropriate for the simulation in the studied species.
- Simulations of single intercepted events are problematic no matter the time step.
- Good model accuracy is from complementation between small and large rainfall events.

GRAPHICAL ABSTRACT

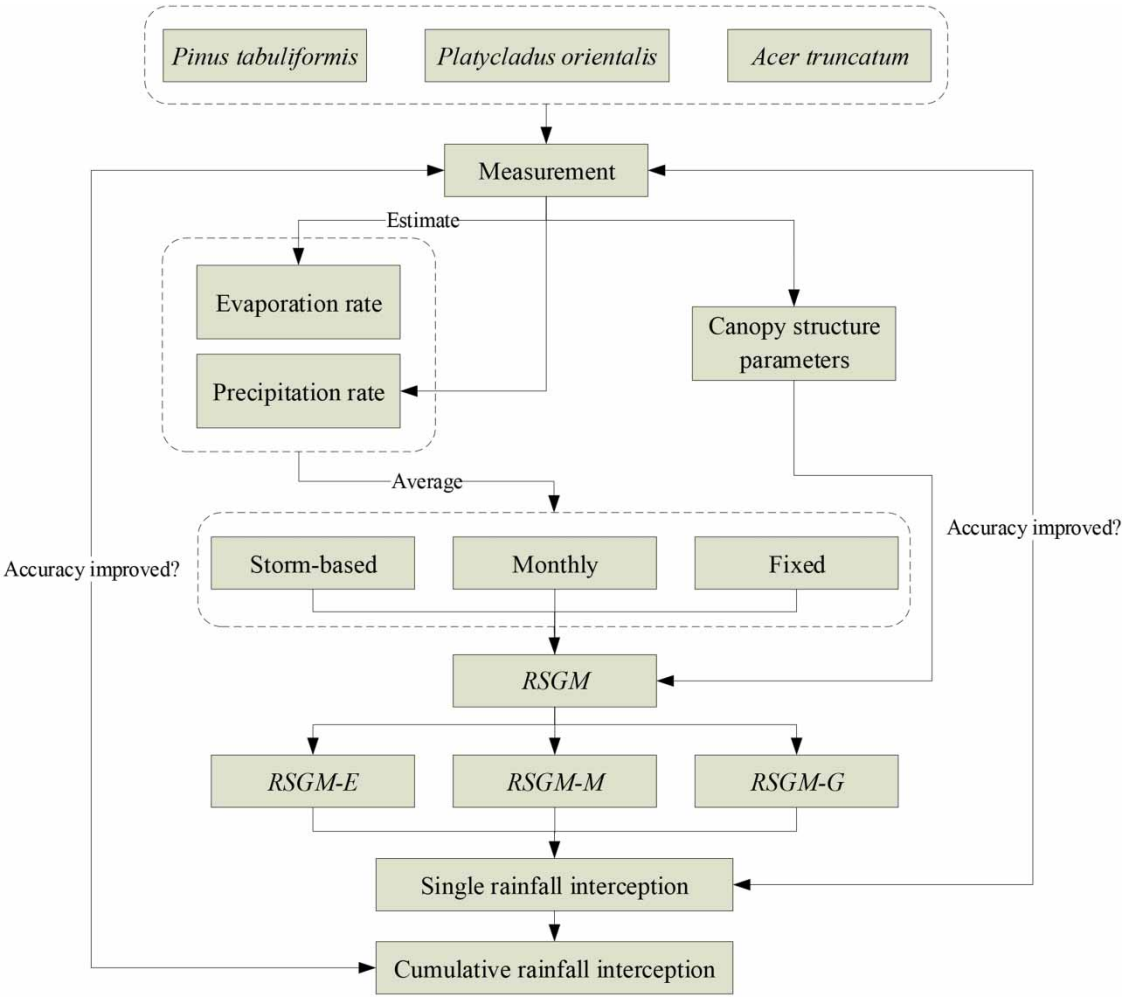

1. INTRODUCTION

Rainfall is a major supply of water within forested catchments and is redistributed into throughfall (*TF*, mm), stemflow (*SF*, mm), and rainfall interception (*I*, mm) after reaching the canopy, thereby affecting the local water balance in a forested ecosystem (Mużyło *et al.* 2012; Ringgaard *et al.* 2014; Sun *et al.* 2014). *I* is defined as precipitation that does not reach the ground, but is rather stored and subsequently evaporated back into the atmosphere from the vegetation canopy, branches, and stems (Price & Carlyle-Moses 2003; Llorens *et al.* 2014; Attarod *et al.* 2015). *I* is, thus, an important component of the forest moisture cycle, with an important influence on the interactions among climate, hydrology, and biology. The amount of *I* is probably greater than that widely estimated (Bulcock & Jewitt 2012), and it has been recognized that *I* can account for a significant percentage of water from forest watersheds (Fan *et al.* 2014; Sadeghi *et al.* 2015), resulting in reduced soil moisture, transpiration, and surface and groundwater recharge (Wallace & McJannet 2006; Linhoss & Siegert 2016). Consequently, accurately identifying and describing the magnitude of *I* is crucial for improving the knowledge of biogeochemical cycling and related hydrological processes (Su *et al.* 2016).

Modeling *I* is an effective method for elucidating the mechanisms of underlying the interception process. The Gash-type models are the most commonly applied approaches (Muzylo *et al.* 2009). The original Gash analytical model (Gash 1979) was proposed to simplify the Rutter model (Rutter *et al.* 1971). It was subsequently reformulated into a sparse version due to its unsuitability for sparse forest stands (Gash *et al.* 1995). Furthermore, Gash model variants have been developed by reformulating parameterization to optimize the model structure for highly accurate simulations of *I* processes. For example, Valente *et al.* (1997) replaced mean evaporation from the saturated canopy ($\bar{E}_c$) in the formula of the sparse Gash model (Gash *et al.* 1995) with $(1 - \varepsilon)\ \bar{E}_c$ (ε, a

constant describing the evaporation rate from saturated trunks as a proportion of that from the saturated canopy, is approximately 0.02). The modeling of *SF* and the calculation of *I* from trunks were also modified, and the results obtained for storms indicated that the relative error in the revised version was approximately 39% lower than that in the original version. The resulting model is referred to as the revised sparse Gash model (RSGM) in this paper. This version appears to be more rigorous in its conceptual and physical approaches than the classical and sparse Gash model. To date, however, there have been few applications of this model version in research relative to the sparse Gash model (Price & Carlyle-Moses 2003; Valente *et al.* 2020).

The stochastic nature of meteorological conditions makes the precise projection of the *I* incident a challenge (Chen *et al.* 2013). To simplify the computational steps as much as possible while maintaining simulation accuracy, Gash (1979) assumed that the average rates of evaporation ($\bar{E}$ or $\bar{E}_c$) and rainfall ($\bar{R}$) during rainfall for saturated canopy conditions are equal for all storms. Subsequently, the hourly values of evaporation rate for saturated canopy conditions over the 4-week period and the entire study period (from 1975 to 1976) were averaged to drive the model separately to examine the assumption, and the validation results indicated that the assumption was justified. Most previous studies have directly accepted this setting (Zhang *et al.* 2018; Lopes *et al.* 2020), employing the Gash model to estimate *I*. However, this assumption has not received sufficient cases for further investigation. Furthermore, variable parameters have been also applied to run the Gash model on an event basis or to calculate the corresponding values of $\bar{E}$ ($\bar{E}_c$) or $\bar{R}$ for single rainfall events. For example, van Dijk & Bruijnzeel (2001a) established equations between $\bar{E}_c$ or the canopy storage capacity (*S*, mm) and the leaf area index (LAI) to dynamically describe the interception characteristics of variable dense vegetation, making corrections to the simulated formula, which resulted in a substantial reduction in the calculated error (van Dijk & Bruijnzeel 2001b). Limousin *et al.* (2008) calculated *I* using the $\bar{E}_c$ and $\bar{R}$ of each rainfall event as inputs, with their outputs agreeing well with the measurements that were underestimated by 6.3%. The above potentially implies that the justification of this assumption in the Gash model has been questioned. Therefore, it is necessary to provide more examples for this assumption to confirm.

Several studies have focused on the accuracy of modeling *I* for individual rainfall events. For example, Fathizadeh *et al.* (2018) used the mean method (Klaassen *et al.* 1998) to separately estimate the corresponding parameters *S* and $\bar{E}_c/\bar{R}$ during the leafed and leafless periods, running the sparse Gash model to calculate the cumulative and single-event interceptions. They obtained a better model performance in the leafed period than in the leafless period. Linhoss & Siegert (2020) compared five canopy interception models (Rutter, Rutter sparse, Gash, sparse Gash, and Liu models) using the Parameter Estimation and Uncertainty Analysis program and the Penman–Monteith equation (Allen *et al.* 1998) between field measurements and predicted individual and cumulative interceptions. They found that the sparse Gash model estimated individual interception poorly and that the modeling accuracy in the leafed period was lower than that in the leafless period. Typically, it was considered that more detailed parameter values for the inputs in the model would result in better estimations. Then, whether the Gash model will be more accurate in estimating *I* for the single storm when the time step of the climate parameter is changed to be storm-based, additional cases are still required to answer this question. Accordingly, the present study, with several plots in the forest stands of *Pinus tabuliformis* (*Pt*), *Platycladus orientalis* (*Po*), and *Acer truncatum* (*At*) in Northern China, was performed to answer the following questions:

1. Is the setting in the Gash model that the climate parameters were equal for all storms correct? Which time-step climate parameters (storm-based, monthly, and fixed) are better for running the RSGM?
2. Does a change in the time step of the climate parameter improve the estimation accuracy of the RSGM of a single *I* event?

2. MATERIALS AND METHODS

2.1. Site description

The research site (Figure 1) is located 8 km northeast of Mount Tai (Northern China) in Yaoxiang National Forest Park (E11° 05′39″–117°09′26″, N36°17′58″–36°20′30″) at an elevation ranging from 400 to 956 m, with a mean elevation of approximately 710 m. The site is located in a warm temperate zone with a semi-humid and monsoon climate, corresponding to a Dwa Köppen climate-type (Zhu & Li 2015; Li & Ye 2019), with a mean annual temperature of 18.5 °C, and a mean yearly frost-free period of 198 days. The multi-year mean precipitation is 727.9 mm, 75% of which occurs from June to September. The soil type is brown soil, and the underlying rock is an ancient gneiss of high metamorphic grade, with an average thickness of 10–90 cm, mostly within 30–50 cm. The vegetation types belong to coniferous and deciduous broad-leaved forests in the warm temperate zone, and the main tree species include *Pt* Carr., *Quercus acutissima* Carr., *Pinus densiflora* Sieb., *Robinia pseudoacacia*, and *Castanea mollissima* (Sun *et al.* 2019).

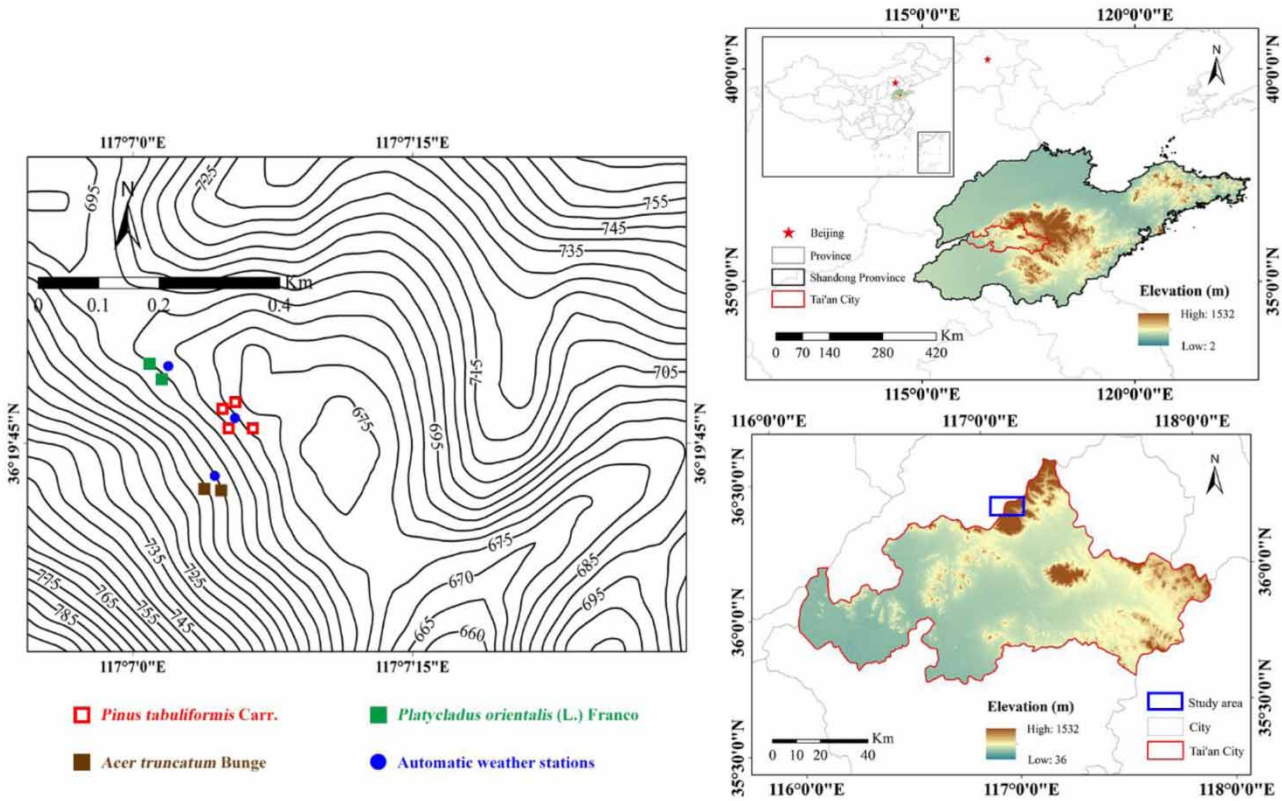

Figure 1 | Study location.

The survey of the forest plots was conducted in March 2017 (Table 1). A total of eight plots (each with a projection area of 100 m^2, a length of 20 m, and a width of 5 m) were set up from September to October 2015 (Figure 1). Four plots were set up for *Pt*, two for *Po*, and two for *At* Bunge, as shown in Table 1. Every tree was the same species on each plot.

2.2. Measurements

Three HOBO automatic weather stations (Onset, Bourne, USA) were installed in the surrounding open area of the plots in March 2016. The so-called open area was an unsheltered area within a radius of at least 5 m, with the automatic weather station at the center. Automatic weather stations were installed separately on a combined structure consisting of a metal pedestal (2 m) and a simple additional mast with height (MH, m). The value of MH was higher by 2 m than the highest tree height (TH, m) within a radius of 10 m from the automatic weather station, i.e., MH = TH + 2. The mast was held firmly in place by

Table 1 | Investigation results of stand plots

Plot	Species	Slope (°)	Stem density (trees ha^{-1})	TDP (trees)	Average height (m)	DBH (cm)
1	*Pt*	23	760	8	10.61 ± 0.43	22.5 ± 0.68
2	*Pt*	24	1,010	12	9.27 ± 0.47	19.2 ± 1.01
3	*Pt*	23	1,695	16	9.38 ± 0.50	17.2 ± 0.82
4	*Pt*	21	2,746	28	12.33 ± 0.59	17.9 ± 0.77
5	*Po*	22	1,563	15	2.54 ± 0.20	3.6 ± 0.11
6	*Po*	23	2,704	28	2.43 ± 0.18	4.0 ± 0.17
7	*At*	23	1,742	18	10.25 ± 0.33	17.2 ± 0.92
8	*At*	25	2,621	27	8.71 ± 0.52	10.4 ± 0.64

Pt = *P. tabuliformis*, *Po* = *P. orientalis*, *At* = *A. truncatum*, DBH = diameter at breast height, *Sp.* = species, TDP = tree density per plot. Data are given as mean ± standard deviation.

four metal chains that were connected to the ground. Data collectors (HOBO U30, Onset; CR1000, Campbell, Logan, USA) were mounted on the top of the metal base, and sensors for air temperature (S-THB, Onset), relative humidity (S-THB-M002, Onset), net radiation (CN1-R, Middleton Solar, Melbourne, Australia), atmospheric pressure (S-BPB-CM50, Onset), and wind speed (S-WSA-M003, Onset) were mounted on the top of the mast. A tipping bucket rain gauge (S-RGB-M002, Onset), with a diameter of 15.2 cm, was also mounted on the top of the mast. It was guaranteed that the total rainfall would not be sheltered and intercepted by the neighboring trees during the measurement process.

Because the distance between each plot of a single tree species was relatively close (<80 m), there was little variation in the climatic conditions, and only one meteorological station was required to be installed at each tree species to collect the necessary data. The weather stations collected data at 15-min intervals. Meteorological data from May–October 2017 as well as observations of rainfall, *I*, *SF*, and *TF* for the corresponding period were selected. Some meteorological data for *At* were lost due to a malfunction of the instrument. However, there was a negligible difference in the meteorological data between *At* and *Po* on comparing the daily monitoring data of the same period (May–October) in 2016 and 2017. Furthermore, the duration of most rainfall events in the two areas is similar, and the frequency of each rainfall event is remarkably consistent. Consequently, after careful consideration, meteorological data for *At* were replaced by those for *Po*, whereas the rainfall data for *At* remained unchanged.

The gross precipitation (P_G, mm) was measured by the automatic weather stations. Referring to previous works (Návar 2013; Ringgaard *et al.* 2014; Ghimire *et al.* 2017), three polyvinyl chloride (PVC) tubes (DN90) with a length of 8 m and an inner diameter of 9 cm were cut open to collect *TF* and distributed under the canopy as much as possible. To avoid the influence of herbs on *TF* collection, the tubes were arranged parallel to the slope along the sample sites, and the height from the collector to the ground was not less than 50 cm (Sheng *et al.* 2014; Ji & Cai 2015), connecting with the collecting barrel at the bottom of the pipes. The volume of water in the collecting barrel was measured after each rainfall event. The tubes were swept after the measurement to ensure that no dead branches, leaves, etc. were present. The collectors remained fixed throughout the study period, and *TF* depth was calculated using the following equation:

$$TF = \frac{1,000 \times V}{L \times W \times \cos\alpha} \tag{1}$$

where *TF* is the throughfall depth (mm), *V* is the water volume collected after each rainfall event (L), *L* is the length of the PVC tube (m), *W* is the inner diameter of the PVC tube (m), and α is the slope of the sample plots (°).

SF was measured by referring to the study of Hanchi & Rapp (1997). Based on the survey results of each plot, the trees were categorized into three classes on the basis of diameter at breast height (DBH) to represent the DBH range of the trees within each plot, and the corresponding number of trees from each class was selected as samples according to the proportion of the total number of trees in each class. A rubber pipe cut in the middle was stapled onto the trunks in a spiral manner. The gap between the rubber pipe and trunk was sealed with silicone, the bottom end of the rubber pipe was connected to a 40-L collecting bucket, and the volume of water collected in the bucket was measured after each rainfall event. *SF* depth was calculated using the following equation (Fan *et al.* 2014):

$$SF_j = \sum_{i=1}^{n} \frac{G_i \cdot M}{K \cdot 10^4} \tag{2}$$

where SF_j is the *j*th events measured *SF* depth (mm), *n* is the number of the corresponding diameter classes (dimensionless; $n = 3$ in this study), G_i is the average *SF* volume collected from *M* trees in each diameter class (ml), *M* is the number of trees in each diameter class (dimensionless), and *K* is the area of the sample plot (m^2).

Based on the water balance of the canopy (Iida *et al.* 2005; Liu *et al.* 2018), the following formula was used to calculate the observed canopy interception (mm):

$$I = P_G - TF - SF \tag{3}$$

A digital single-lens reflex camera (EOS 90D, Canon, Japan) was used to acquire hemispherical photographs, which were processed using Adobe Photoshop software (cc2015, Adobe Systems Software Ireland Ltd, San Jose, USA) to obtain canopy

cover fraction (c, dimensionless), and 12 photos were taken for each plot during the study period. Considering that the period of this study was only the growing season, the canopy structure of deciduous and evergreen species remained almost unchanged. Therefore, c was averaged for each plot during the study period to be used as a model input parameter.

2.3. Model expression

This study used a simplified RSGM on the basis of studies by Valente *et al.* (1997) and Limousin *et al.* (2008), such that the I of each rainfall event was calculated as shown in Table 2. S was estimated using the regression method proposed by Leyton *et al.* (1967), which is based on the relationship between P_G and TF. Drainage partitioning coefficient (p_t, dimensionless) and trunk storage capacity (S_t, mm) were deduced based on the relationship between P_G and SF (Gash 1979). To further demonstrate the direct effect of meteorological parameters on model accuracy, S, S_t, c, and p_t were used as fixed values to run the model, regardless of versions, which is permissible for the operation of the model (Valente *et al.* 2020).

The evaporation rate from the canopy (E_c, mm) was calculated using the Penman–Monteith equation, and aerodynamic conductance was estimated using Equation (5), assuming that the canopy resistance was set to zero (Gash 1979):

$$E_c = \frac{\Delta R_n + \rho c_p r_a}{\lambda(\Delta + \gamma)} \tag{4}$$

where Δ is the slope of saturation vapor pressure versus temperature curve (kPa K^{-1}), R_n is the net radiation (W m^{-2}), ρ is the air density (kg m^{-3}), c_p is the specific heat of air (J kg^{-1} K^{-1}), λ is the latent heat of vaporization of water (kPa K^{-1}), γ is the psychometric constant (J kg^{-1}), and r_a is the aerodynamic conductance (m s^{-1}), which is estimated as follows:

$$r_a = \frac{k^2 u}{\ln\left[(z-d)/z_0\right]^2} \tag{5}$$

where k is the von Kármán constant (dimensionless, here 0.41), u is the wind speed at height z (m), z is the reference height above the ground surface (here the height of the wind speed and relative humidity measurement in this study [m]), d is the zero-plane displacement height (m, here assumed to be 0.7 h, where h is the canopy height), and z_0 is the roughness length for momentum (m, here assumed to be 0.1 h).

The amount of rain necessary to saturate the canopy (P'_G) was determined using Equation (6). The amount of rainfall necessary to saturate the trunks was calculated using Equation (7) and is denoted as P''_G (Valente *et al.* 1997; Limousin *et al.* 2008):

$$P'_G = -\frac{\bar{R}}{\bar{E}_c} S_c \ln\left[1 - \frac{\bar{E}_c}{\bar{R}}\right] \tag{6}$$

$$P''_G = \left(\frac{\bar{R}}{\bar{R} - \bar{E}_c}\right)\left(\frac{S_t}{p_t c}\right) + P'_G \tag{7}$$

Assuming that hours with $P_G > 0.4$ mm represent saturated canopy conditions (Valente *et al.* 1997; Mużyło *et al.* 2012), the hourly values of E_c were calculated by Equation (4), and subsequently three versions of the RSGM were run defined in this study. RSGM-E was defined as that the hourly values of E_c for saturated canopy conditions were averaged over the storm period to obtain the estimate of $\bar{E}_c$ to drive the RSGM, and these hourly P_G were extracted and averaged over the same period to obtain $\bar{R}$, i.e., $\bar{E}_{c,j}$ and $\bar{R}_j$ were substituted for the corresponding $\bar{E}_c$ and $\bar{R}$ in Equations (6)–(7), respectively. Likewise, RSGM-M was defined as that running the RSGM using the monthly climatic parameters, and RSGM-G was defined as the RSGM run with the averaged E_c and rainfall rates over the whole growing season under saturated canopy conditions. All three versions were based on independent rainstorms for calculating I. In the present study, independent rain events were defined such that each storm was separated by at least an 8-h rain-free period.

2.4. Model performance analysis

Because the number of rainfall events per plot is small, leave-one-out cross-validation was used in this study with reference to the research conducted by Fathizadeh *et al.* (2018). This approach is consistent in principle with the most common approach

Table 2 | Comparison of the components in the original Gash model with those of some RSGMs

	Original version	Revised version		
	Gash (1979)	Gash *et al.* (1995)	Valente *et al.* (1997)	This study
For m small storms insufficient to saturate the canopy	$(1-p-p_t)\sum_{j=1}^{m} P_{G,j}$	$c\sum_{j=1}^{m} P_{G,j}$	$c\sum_{j=1}^{m} P_{G,j}$	$c\sum_{j=1}^{m} P_{G,j}$
Wetting up the canopy, for n storms that saturate the canopy	$n(1-p-p_t)P'_G - nS$	$cnP'_G - ncS_c$	$cnP'_G - ncS_c$	$c\sum_{j=1}^{n} P'_{G,j} - c\sum_{j=1}^{n} S_c$
Evaporation from saturation until rainfall ceases	$\frac{\bar{E}}{\bar{R}}\sum_{j=1}^{n}(P_{G,j}-P'_G)$	$\frac{c\bar{E}_c}{\bar{R}}\sum_{j=1}^{n}(P_{G,j}-P'_G)$	$\frac{c(1-\varepsilon)\bar{E}_c}{\bar{R}}\sum_{j=1}^{n}(P_{G,j}-P'_G)$	$\sum_{j=1}^{n}\left(\frac{c\bar{E}_c}{\bar{R}}\right)(P_{G,j}-P'_{G,j})$
Evaporation after rainfall ceases	nS	ncS_c	ncS_c	ncS_c
For $m+n-q$ (original version) or $n-q$ (revised version) storms that do not saturate the trunks	$qS_t + p_t\sum_{j=1}^{n+m-q} P_{G,j}$	$qS_t + p_t\sum_{j=1}^{n-q} P_{G,j}$	$qS_t + p_d c\left[1-\frac{(1-\varepsilon)\bar{E}_c}{\bar{R}}\right]\sum_{j=1}^{n}(P_{G,j}-P'_G)$	$qS_t + cp_t\sum_{j=1}^{n-q}\left(1-\frac{\bar{E}_c}{\bar{R}}\right)(P_{G,j}-P'_{G,j})$
SF	$p_t\sum_{j=1}^{q} P_{G,j} - qS_t$	$p_t\sum_{j=1}^{q} P_{G,j} - qS_t$	$p_d c\left[1-\frac{(1-\varepsilon)\bar{E}_c}{\bar{R}}\right]\sum_{j=1}^{q}(P_{G,j}-P'_G) - qS_t$	$cp_t\left(1-\frac{\bar{E}_c}{\bar{R}}\right)\sum_{j=1}^{q}(P_{G,j}-P'_{G,j}) - qcS_t$
TF	$p\sum_{j=1}^{m+n} P_{G,j} + \left[(1-p-p_t)-\frac{\bar{E}}{\bar{R}}\right]\sum_{j=1}^{n}(P_{G,j}-P'_G)$	$\sum_{j=1}^{n+m} P_{G,j} - \sum_{j=1}^{n+m} I_j - \sum_{j=1}^{q} SF_j$	$(1-c)\sum_{j=1}^{m+n} P_{G,j} + c(1-p_d)[1-\frac{(1-\varepsilon)\bar{E}_c}{\bar{R}}]\sum_{j=1}^{n}(P_{G,j}-P'_G)$	$\sum_{j=1}^{n+m} P_{G,j} - \sum_{j=1}^{n+m} I_j - \sum_{j=1}^{q} SF_j$

m = number of small storms insufficient to saturate the canopy (dimensionless), j = number of rainfall events, p = free throughfall coefficient (dimensionless), p_t and p_d = drainage partitioning coefficient (dimensionless), n = number of storms sufficient to saturate the canopy (dimensionless), P'_G = amount of rain necessary to saturate the canopy (mm), S = canopy storage capacity per unit ground area (mm), P_G = amount of total rainfall (mm), $\bar{E}$ = mean evaporation for saturated canopy conditions (mm h^{-1}), $\bar{R}$ = mean rainfall rate for saturated canopy conditions (mm h^{-1}), q = number of storms that saturate trunks (dimensionless), S_t = trunk storage capacity (mm), SF = stemflow (mm), TF = throughfall (mm), c = canopy cover fraction (dimensionless), S_c = canopy capacity per unit area of cover (mm), $S_c = S/c$, $\bar{E}_c$ = mean evaporation rate from the saturated canopy (mm h^{-1}), I = rainfall interception (mm), $\varepsilon = 0.02$, a constant describing the evaporation rate from saturated trunks as a proportion of that from the saturated canopy.

of generating parameters with half of the data and testing the model on the other half, assuming that the original data has N samples (here N for *Pt* is 25 and N for *At* and *Po* is 28), each sample individually as the validation set, and the remaining $N-1$ samples as the training set. Several common quantitative methods were applied to determine model performance. All statistical indicators in this work were the mean of the validation set, and the presented estimations of *I*, *SF*, and *TF* were also the validation set.

The absolute percentage error (*APE*), the mean absolute error (*MAE*), the absolute error (*AE*), the root-mean-squared error (*RMSE*), and the Nash–Sutcliffe efficiency coefficient (*NSE*) are employed to evaluate model performance (Amiri-Ardakani & Najafzadeh 2021; Najafzadeh *et al.* 2021), and they are described as follows:

$$APE = \frac{\left|\sum_{i=1}^{N} P_i - \sum_{i=1}^{N} Q_i\right|}{\sum_{i=1}^{N} Q_i} \times 100\%, \quad 0\% \le APE < +\infty \tag{8}$$

where P_i is the predicted interception value (mm), Q_i is the observed interception value (mm), and N is the number of observed events (dimensionless).

$$MAE = \frac{\sum_{i=1}^{N} |P_i - Q_i|}{N}, \quad 0 \le MAE < +\infty \tag{9}$$

$$AE = \left|\sum_{i=1}^{N} P_i - \sum_{i=1}^{N} Q_i\right|, \quad 0 \le AE < +\infty \tag{10}$$

$$RMSE = \sqrt{\frac{\sum_{i=1}^{N} (P_i - Q_i)^2}{N}}, \quad 0 \le RMSE < +\infty \tag{11}$$

$$NSE = 1 - \frac{\sum_{i=1}^{N} (Q_i - P_i)^2}{\sum_{i=1}^{N} (Q_i - \bar{Q})^2}, \quad -\infty \le NSE \le 1 \tag{12}$$

where $\bar{Q}$ is the average observed value of I (mm).

2.5. Sensitivity analysis

The local sensitivity analysis technique was used in this study to assess parameter importance (Fathizadeh *et al.* 2018; Ma *et al.* 2020). The original values of S, S_t, p_t, c, $\bar{R}$, and $\bar{E}_c$ were increased and decreased by 10% from −50 to 50%, and the results of running the model were compared with field-measured values. When RSGM-E was tested for sensitivity, the $\bar{R}$ or $\bar{E}_c$ of all single rainfall events was increased or decreased together. However, for RSGM-M, the monthly average values of $\bar{R}$ or $\bar{E}_c$ were treated as a whole (increased or decreased).

3. RESULTS

3.1. Rainfall partitioning

In total, 25, 28, and 28 events were monitored for *Pt*, *Po*, and *At*, with a total rainfall of 427.2 mm ($P_{G,\,Pt}$), 490.1 mm ($P_{G,\,Po}$), and 497.2 mm ($P_{G,\,At}$), respectively. The cumulative I increased in the same species with the planting densities increased, amounting to 59.7 mm in plot 1 (14.0% of $P_{G,\,Pt}$), 84.2 mm in plot 2 (20.7% of $P_{G,\,Pt}$), 96.8 mm in plot 3 (22.7% of $P_{G,\,Pt}$), and 115.9 mm in plot 4 (27.1% of $P_{G,\,Pt}$); 88.2 mm in plot 5 (18.0% of $P_{G,\,Po}$) and 100.8 mm in plot 6 (20.6% of $P_{G,\,Po}$); and 60.7 mm in plot 7 (12.2% of $P_{G,\,At}$) and 72.6 mm in plot 8 (14.6% of $P_{G,\,At}$).

3.2. Results of RSGM application

The parameters that were used for the model calculations are presented in Table 3. Three model versions underestimated the accumulated *I* in all plots. However, the estimated results by RSGM-G were closer to the observed interception for all species, whereas the deviation of RSGM-E was the greatest (Figure 2). Overall, larger underestimations were obtained for RSGM-E, with 12.9–20.7% for *Pt*, 16.4–16.5% for *Po*, and 14.0–14.7% for *At*, whereas better fits were obtained for RSGM-G, in which cumulative *I* were underestimated by 9.9–16.1% for *Pt*, 13.6–15.9% for *Po*, and 15.7–20.2% for *At*. Moreover, differences were found between the estimated results of RSGM-M and RMGM-G, ranging from 0.13 to 0.34 mm.

All model versions showed poor variable accuracy in simulating the interceptions of individual rainfall events, irrespective of the tree species. More deviations occurred in certain small storms and large storms, which were correspondingly overestimated and underestimated (Figure 3).

As shown in Table 4, most *I* evaporated from the saturated canopy after the rainfall ceased. This component exceeded 50% of the total calculated volume of the *I*, regardless of the model version and tree species, ranging between 67.2 and 81.0%. The

Table 3 | Summary of model parameters for the calculation

Tree species	Plot	S (mm)	S_t (mm)	p_t (–)	c (–)	$\bar{R}$ (mm h^{-1})	$\bar{E}_c$ (mm h^{-1})
Pt	1	1.666	0.044	0.007	0.74	2.02	0.0582
Pt	2	2.461	0.370	0.061	0.75	2.02	0.0581
Pt	3	2.959	0.474	0.083	0.78	2.02	0.0578
Pt	4	3.845	0.426	0.077	0.78	2.02	0.0584
Po	5	2.449	0.103	0.029	0.74	1.75	0.0577
Po	6	2.880	0.291	0.063	0.78	1.75	0.0576
At	7	1.357	0.043	0.057	0.73	1.78	0.0592
At	8	1.887	0.050	0.043	0.76	1.78	0.0590

Pt = *Pinus tabuliformis*, *Po* = *Platycladus orientalis*, *At* = *Acer truncatum*, S = canopy storage capacity, S_t = trunk storage capacity, p_t = drainage partitioning coefficient, c = canopy cover fraction, $\bar{R}$ = mean rainfall rate for saturated canopy conditions, $\bar{E}_c$ = mean evaporation rate from the saturated canopy.

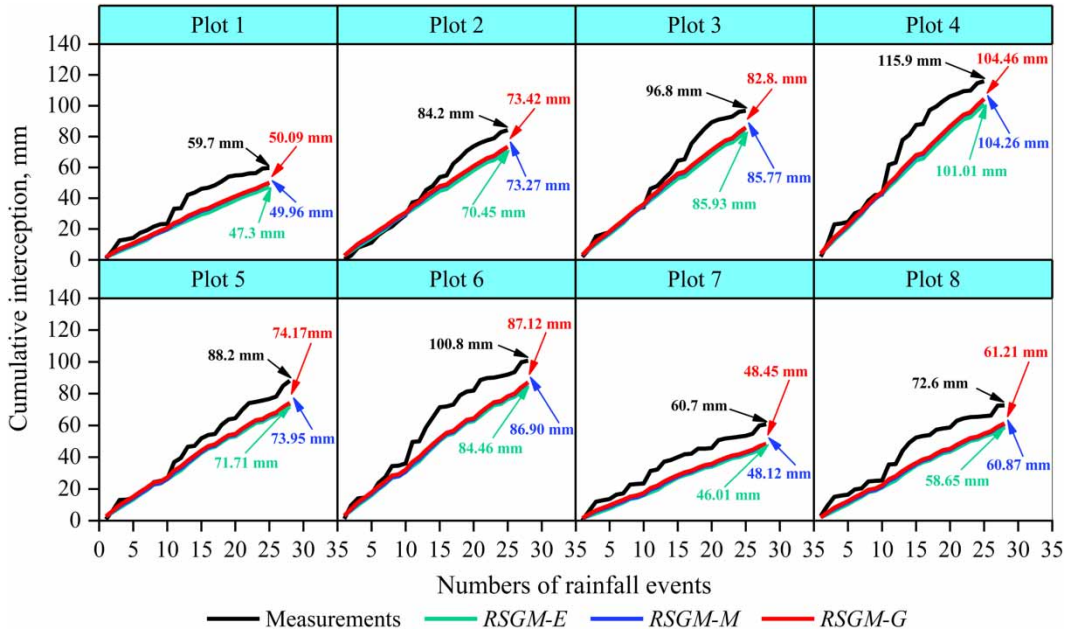

Figure 2 | Comparison among three versions of the modeled interception for each plot. The tree species in plots 1–4 are *Pt*, those in plots 5 and 6 are *Po*, and those in plots 7 and 8 are *At*. Arabic numerals appended to the arrowed lines represent cumulative interception values computed by different versions of the model.

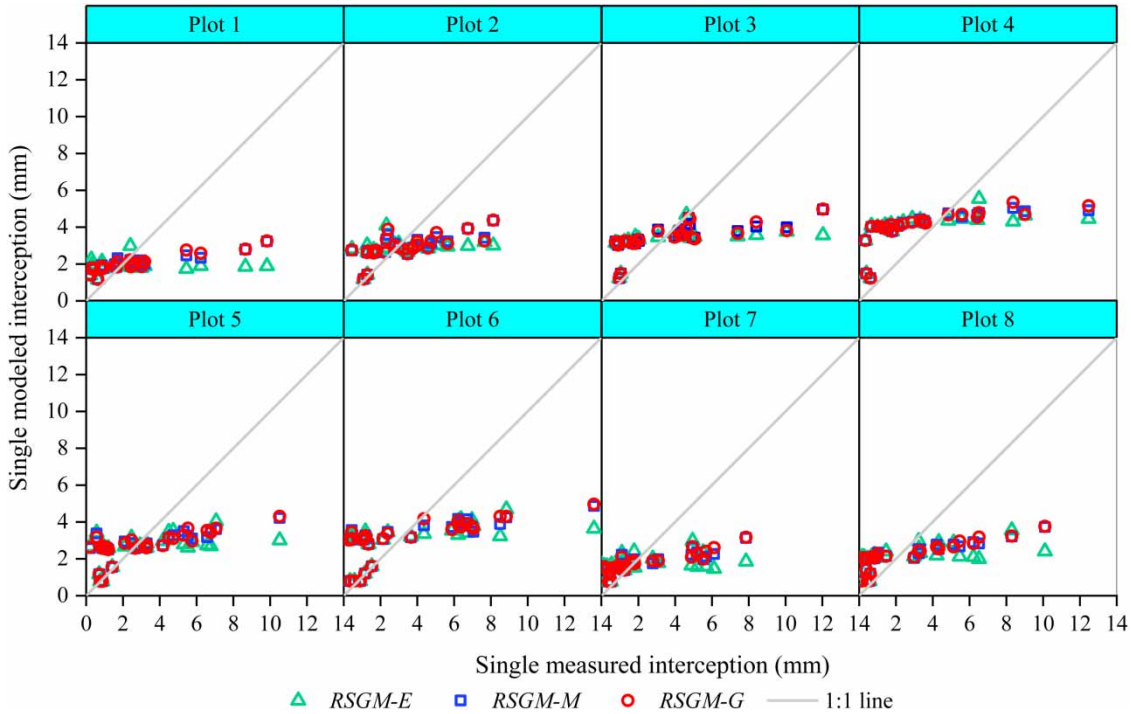

Figure 3 | Modeled interception by three versions of the model versus those measured for single rainfall events. Each dot represents a rainfall event. The tree species in plots 1–4 are *Pt*, those in plots 5 and 6 are *Po*, and those in plots 7 and 8 are *At*.

lowest losses were derived from n storms that saturated the canopy, ranging between 1.1 and 1.7%. The increase in evaporation from saturation until the rainfall ceased was the primary reason for the difference in calculation among the models. In the same plots, the maximum value was usually calculated by the RSGM-G model, followed by the RSGM-M and RSGM-E models.

3.3. Prediction accuracy

Five statistical indexes for the different model versions are presented in Table 5. As shown, the *APE*, *AE*, *RMSE*, and *MAE* values for RSGM-G were lower than those for RSGM-M in all plots, followed by those for RSGM-E. The opposite trend is observed in other indexes.

The reduction in *RMSE*, *MAE*, *APE*, and *AE* values for RSGM-G compared with those for RSGM-E did not exceed 22.4% (for *Pt*), 15.7% (for *Po*), and 17.4% (for *At*) but was no more than 1.6% (for *Pt*), 1.7% (for *Po*), and 2.8% (for *At*) compared with those for RSGM-M. The mean *NSE* values for RSGM-G were 0.21 (for *Pt*), 0.15 (for *Po*), and 0.22 (for *At*) higher compared with those for RSGM-E, whereas the values varied slightly compared with those for RSGM-M in all tree species. In general, RSGM-G exhibited superior performance relative to RSGM-M and RSGM-E for all species.

Differing model performances according to the tree species depended on the type of statistical indexes and stem densities used. For example, when using *APE*, on the premise of a density of approximately 1,600 or 2,700 trees ha^{-1}, for all models, the most accurate predictions were obtained for *Pt*. However, all the models generated the best estimation of I for *At* when *RMSE* and *MAE* were used for a density of approximately 1,600 or 2,700 trees ha^{-1}.

3.4. Sensitivity analysis

Sensitivity analyses for six parameters (S, S_t, p_t, c, $\bar{R}$, and $\bar{E}_c$) were conducted to determine their influence on the predicted I and assess differences between the models (Figure 4). In general, $\bar{R}$ showed a negative correlation with the cumulative interception throughout all tested parameters, whereas the other parameters showed an opposite trend (Liu *et al.* 2018; Lopes *et al.* 2020; Ma *et al.* 2020).

S was the main sensitive parameter that influenced interception prediction when the tested parameter changes were in the $\pm$50% range, regardless of the model used and the tree species. The interception was less sensitive to parameters p_t and

Table 4 | Five components of rainfall interception calculated by three versions of the model (*RSGM-E*, *RSGM-M*, and *RSGM-G*)

	Pt				*Po*		*At*	
	Plot 1	**Plot 2**	**Plot 3**	**Plot 4**	**Plot 5**	**Plot 6**	**Plot 7**	**Plot 8**
	RSGM-E							
1. For *m* small storms, insufficient to saturate the canopy, mm	2.57	2.61	2.71	13.88	5.06	8.00	4.84	5.04
2. Wetting up the canopy, for *n* storms that saturate the canopy, mm	0.79	1.16	1.39	1.19	1.12	1.17	0.61	0.85
3. Evaporation from saturation until rainfall ceases	4.89	4.23	4.01	3.30	7.26	7.14	8.34	8.23
4. Evaporation after rainfall ceases	38.31	56.60	68.06	76.90	56.33	63.36	31.22	43.39
5. Evaporation from trunks	0.74	5.85	6.62	5.74	1.94	4.80	0.99	1.14
Cumulative simulated *I*, mm	47.30	70.45	82.80	101.01	71.71	84.46	46.01	58.65
Cumulative simulated *SF*, mm	1.61	14.40	18.10	17.22	9.52	19.22	23.81	16.92
Cumulative simulated *TF*, mm	378.27	342.34	326.29	308.96	408.85	386.40	427.38	421.63
	RSGM-M							
1. For *m* small storms, insufficient to saturate the canopy, mm	2.57	2.61	2.71	9.77	5.06	8.00	3.46	5.04
2. Wetting up the canopy, for *n* storms that saturate the canopy, mm	0.79	0.87	1.05	1.25	0.95	1.07	0.55	0.73
3. Evaporation from saturation until rainfall ceases	4.89	7.28	7.26	6.72	9.66	9.64	10.54	10.58
4. Evaporation after rainfall ceases	38.31	56.60	68.06	80.75	56.33	63.36	32.58	43.39
5. Evaporation from trunks	0.74	5.91	6.69	5.78	1.95	4.83	0.99	1.14
Cumulative simulated *I*, mm	49.96	73.27	85.77	104.26	73.95	86.90	48.12	60.87
Cumulative simulated *SF*, mm	1.59	14.17	17.80	16.93	9.45	19.03	23.69	16.83
Cumulative simulated *TF*, mm	375.64	339.75	323.61	306.00	406.68	384.15	425.39	419.50
	RSGM-G							
1. For *m* small storms, insufficient to saturate the canopy, mm	2.57	2.61	2.71	9.77	5.06	8.00	3.46	5.04
2. Wetting up the canopy, for *n* storms that saturate the canopy, mm	0.56	0.83	0.99	1.19	0.95	1.07	0.55	0.74
3. Evaporation from saturation until rainfall ceases	7.89	7.47	7.47	6.97	9.88	9.87	10.87	10.90
4. Evaporation after rainfall ceases	38.31	56.60	68.06	80.75	56.33	63.36	32.58	43.39
5. Evaporation from trunks	0.75	5.91	6.70	5.79	1.95	4.83	0.99	1.14
Cumulative simulated *I*, mm	50.09	73.42	85.93	104.46	74.17	87.12	48.45	61.21
Cumulative simulated *SF*, mm	1.59	14.16	17.78	16.90	9.44	19.02	23.68	16.82
Cumulative simulated *TF*, mm	375.51	339.61	323.48	305.82	406.46	383.94	425.08	419.17

n = number of storms sufficient to saturate the canopy, *m* = number of small storms insufficient to saturate the canopy, *I* = rainfall interception, *SF* = stemflow, *TF* = throughfall.

S_t, which presented changes smaller than ± 2.0 and ± 3.1%, respectively. Moreover, $\bar{E}_c$ was the second most sensitive parameter when changed from 0 to 50%, leading to a change in cumulative *I* of approximately 8.4, 7.3, and 11.8% for *Pt*, *Po*, and *At*, respectively. In contrast, $\bar{R}$ was the second most sensitive parameter in the range from −50 to 0%, resulting in variations of 16.8, 14.5, and 23.5% for *Pt*, *Po*, and *At*, respectively.

The effects of $\bar{E}_c$ and $\bar{R}$ showed increases with the temporal scale of calculation of the meteorological parameters within the same plots, whereas *S*, S_t, and p_t showed the opposite trend. For example, a 50% increase or decrease in *S* caused the cumulative interception predicted by RSGM-E to change within an average range from −40.7 to 39.5% for *Pt*, and from −39.3 to 37.6%, and from −39.3 to 37.5% for RSGM-M and RSGM-G, respectively. Conversely, $\bar{E}_c$ increased to 50% for *Pt*, resulted in simulated interception increases of an average of 5.7% for RSGM-G, by 5.6% for RSGM-M, and by 3.7% for RSGM-E.

4. DISCUSSION

The value of $\bar{E}_c$ was reported to be quite conservative among regions and species, ranging from 0.2 to 0.4 mm h^{-1} (Miralles *et al.* 2010). However, in the present study, the $\bar{E}_c$ values used to run RSGM-G in each plot were considerably smaller. The $\bar{E}_c$ values involved in the model operations reported by Miralles *et al.* (2010) were derived from other reference values, related to

Table 5 | Five indexes for the three model versions (RSGM-E, RSGM-M, and RSGM-G) used to evaluate the performance of the estimated rainfall interception

		RSGM-E					RSGM-M					RSGM-G				
Tree species	**Plot**	***NSE***	***RMSE***	***MAE***	***APE* (%)**	***AE* (mm)**	***NSE***	***RMSE***	***MAE***	***APE* (%)**	***AE* (mm)**	***NSE***	***RMSE***	***MAE***	***APE* (%)**	***AE* (mm)**
Pt	1	−0.04	2.57	1.70	20.73	12.37	0.24	2.20	1.49	16.29	9.72	0.26	2.16	1.46	16.07	9.59
Pt	2	0.05	1.99	1.50	16.33	13.75	0.29	1.72	1.35	12.98	10.93	0.31	1.70	1.33	12.80	10.78
Pt	3	0.11	2.77	1.97	14.45	13.99	0.27	2.51	1.82	11.38	11.01	0.27	2.51	1.81	11.22	10.86
Pt	4	0.11	4.50	3.10	12.86	14.91	0.24	4.16	2.93	10.05	11.66	0.25	4.14	2.91	9.88	11.45
Po	5	0.16	2.34	1.68	18.67	16.46	0.33	2.09	1.56	16.12	14.22	0.34	2.06	1.55	15.87	14.00
Po	6	0.22	3.00	2.37	16.22	16.36	0.32	2.81	2.17	13.81	13.92	0.33	2.78	2.16	13.59	13.71
At	7	0.07	2.14	1.55	24.26	14.74	0.30	1.87	1.38	20.79	12.63	0.33	1.82	1.36	20.24	12.30
At	8	0.17	2.46	1.85	19.25	13.98	0.33	2.22	1.74	16.19	11.76	0.34	2.19	1.72	15.73	11.43

Pt = *P. tabuliformis*, *Po* = *P. orientalis*, *At* = *A.truncatum*, *NSE* = Nash–Sutcliffe efficiency coefficient, *RMSE* = root-mean-squared error, *MAE* = mean absolute error, *APE* = absolute percentage error of cumulative interception, *AE* = absolute error of cumulative interception.

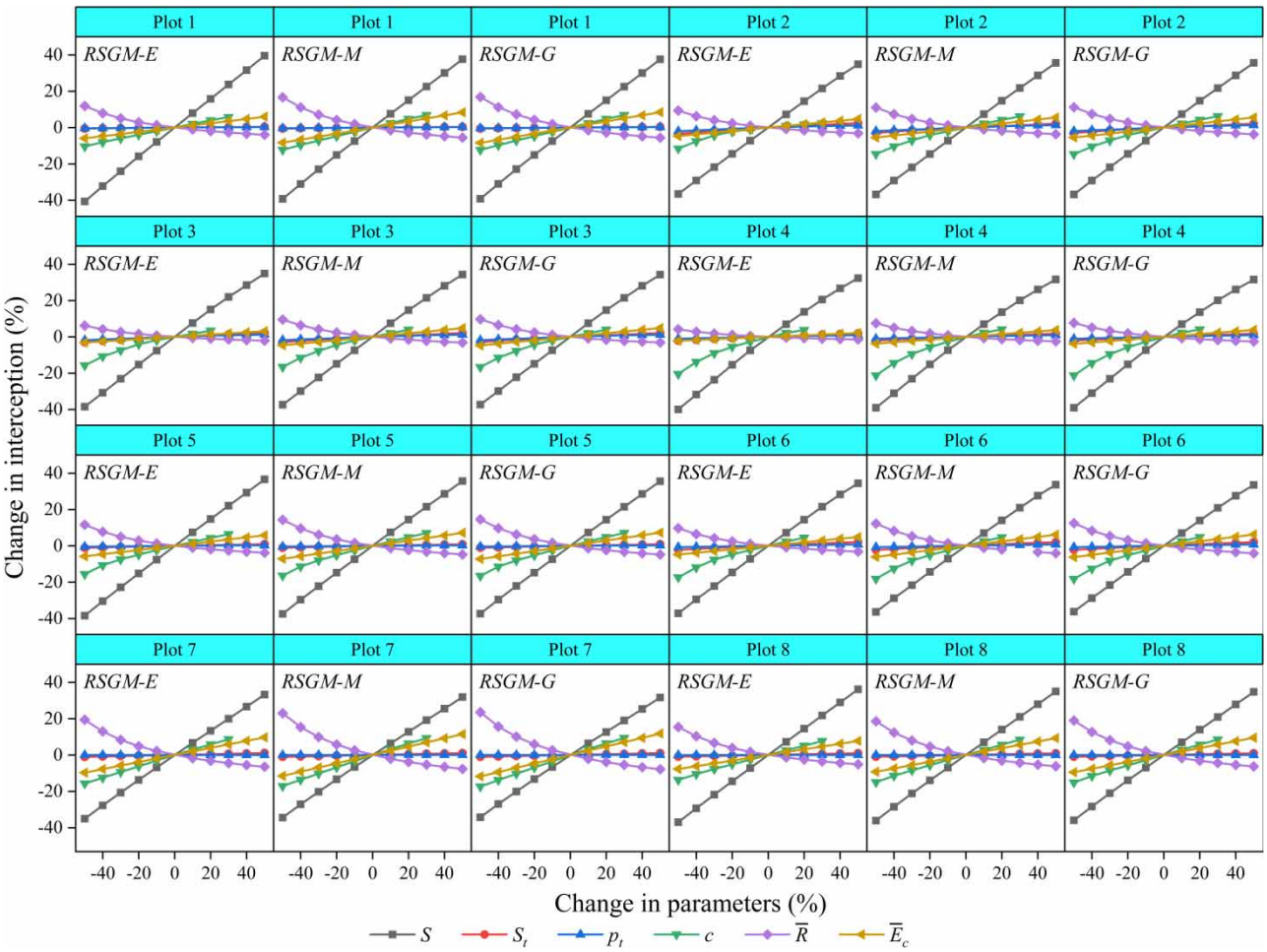

Figure 4 | Sensitivity analysis for the three versions of the RSGM (RSGM-E, RSGM-M, and RSGM-G) for a change in predicted *I*. The tree species in plots 1–4 are *Pt*, those shown in plots 5 and 6 are *Po*, and those shown in plots 7 and 8 are *At*. S = canopy storage capacity (mm), $\bar{R}$ = mean rainfall rate for saturated canopy conditions (mm h^{-1}), c = canopy cover fraction (dimensionless), $\bar{E}_c$ = mean evaporation rate from the saturated canopy (mm h^{-1}), S_t = stem storage capacity (mm), and p_t = drainage partitioning coefficient (dimensionless).

experiments conducted in Britain, Amazonia, Netherlands, Bordeaux (France), Portugal, Mediterranean mountainous area, Puerto Rico, and Mississauga (Ontario, Canada). Therefore, differences in climatic conditions owing to interregional variability probably explain the small $\bar{E}_c$ value in this study (approximately 0.06 mm h^{-1}). Moreover, monitored data measured in the scope of this research were reexamined and showed that most of the rainfall events occurred at night and were rarely accompanied by strong winds, which may have contributed to the relatively small $\bar{E}_c$. Furthermore, the $\bar{E}_c$ values in this study were compared with those obtained in recent studies conducted in China (Shinohara *et al.* 2015; Liu *et al.* 2018; Ma *et al.* 2019, 2020), the observed $\bar{E}_c$ values ranged between 0.01 and 0.10 mm h^{-1}, and the difference between them and this study is not large, indicating the potential correctness of the results in this study. Ghimire *et al.* (2017) used the Penman–Monteith equation and calculated an $\bar{E}_c$ value of 0.07 and 0.08 mm h^{-1} for modeling *I* in two differently aged secondary forests in Madagascar. Moreover, the higher *S*-values of *Pt* (3.845 mm, plot 4) have been explained in previous work (Li *et al.* 2020), and it can be explained by the large stem density in this study and the special plant physiology structure of *Pt*. *S*-values for the other plots were within the range previously reported (Llorens & Gallart 2000; Deguchi *et al.* 2006).

Muzylo *et al.* (2009) summarized studies published before March 2008 regarding *I* modeling. They found that the *APE* range of the sparse Gash model (Gash *et al.* 1995) was mostly less than 20%, whereas the ranges of *APE* in the present study also were in this interval for most sites regardless of the model versions, except for the use of all versions in plot 7 and RSGM-E in plot 1. This indicated that the cumulative annual interception could be accurately calculated by all three model versions (*APE* in the range of 9.9–24.3%). Furthermore, a negative *NSE* value was obtained by running RSGM-E in plot 1. This observation is different from those of studies by Hassan *et al.* (2017) and Fathizadeh *et al.* (2018) and similar to those by Krause *et al.* (2005) and Shi & Wang (2020). However, Equation (13) indicates that a range of *NSE* less than zero is entirely possible, as long as the top of the fraction is greater than the bottom, although it has been claimed to range from 0 to 1 (Sadeghi *et al.* 2015; Lopes *et al.* 2020).

The model framework of the three versions in this study is a combination of those proposed by Valente *et al.* (1997) and Limousin *et al.* (2008). Given that the former proposed model has relatively few applications in forest trees, the results of the present study were compared with those of the other studies using the latter model, and the *APE* values in this study were found to be higher than those reported in previous studies (Zhao *et al.* 2011; Liu *et al.* 2015, 2018). The differences among the tree species, stand density, and even the application mode could be responsible for this. Differences in tree species could cause variation in the canopy structure, concomitantly influencing the simulation of canopy interception. Fathizadeh *et al.* (2017) demonstrated strong relations of *I* and *S* with *c*, the LAI, and the wood area index. However, only *S* and *c* were used in the RSGM to characterize the canopy structure of the plant upper space, which is far from sufficient for tree species with a more complex canopy structure. The addition of forest structure parameters (branch inclination, stem length, bark characteristics, leaf shape, and forest age) to canopy interception models tends to more accurately reveal how changes in tree species affect model simulations and better indicate the differences in ecohydrological components under different canopy structures.

Finally, the distinction in the model application mode can be considered as the fundamental cause of differences in *APE* between the present study and previous works. In this study, the RSGM was run on an event basis, to estimate the cumulative *I* even when fixed climatic parameters were used, rather than directly calculating total *I* (Liu *et al.* 2015). The application mode used in the latter approach may allow annual total *I* to be determined more accurately. However, it is not possible to elaborate on the variations in the canopy water flux for a single interception event. This mode may be successful in simplifying modeling and exploring gross interception, because *I* is most often estimated over a season or a year, instead of a single rainfall event (Fan *et al.* 2014). Model applications with simplified parameters would thus be useful (Mużyło *et al.* 2012), but their validity in terms of physical and practical aspects remains to be discussed. Besides, comparing the use of different models to determine the best combination of model type, application environment (region, species, dormant or growing season, and rainfall patterns), and usage mode will facilitate the development of Gash-type models.

In general, the operational performance of RSGM-G for calculating cumulative *I* was clearly superior to that of RSGM-E, and slightly better than that of RSGM-M. This implies that using constant climatic parameter values in the RSGM to simulate the cumulative canopy interception on the basis of single events during the growing season in the studied region and considering the studied tree species could lead to better performance. A part of these results contradicts those reported by Jackson (2000), who applied the sparse Gash model to single trees using long-term (3 years) and monthly $\bar{R}$ separately to estimate the gross interception and found that the error of the former exceeded that of the latter. This could result from a difference in the

length of the simulated period. Furthermore, in this study, the total interception during the study period was estimated on an event basis, regardless of the model version used, rather than on a month-to-month basis as reported by Jackson (2000). Moreover, previous research focused only on the effects of time-step variability in the rainfall rate and neglected the consideration of the evaporation rate. The combined efforts of those parameters may lead to more complex effects and, subsequently, reduce the error, as noted in the present study.

Changes in seasons and weather patterns may also result in changing climatic and canopy parameters, and subsequent errors would be counteracted in model calculations. Thus, the modeled errors of annual interception using fixed parameters are considered to be minimal, as explained by Wallace & McJannet (2008), Ghimire *et al.* (2012), and Fan *et al.* (2014). However, in the present study, canopy parameters in the RSGM (S and c) were fixed regardless of the model version used, because the study period of the present research is the growing season rather than the entire year. Therefore, the satisfactory performance of RSGM-G in calculating the cumulative interceptions was considered to arise from the mutual compensation between the overestimation of smaller rainfall events and the underestimation of larger rainfall events (Figure 3). Simultaneously, an unknown mutual compensation between climatic parameters might occur during the modeling process, and this effect is not from the climate and canopy parameters as previously reported, because the canopy parameters were fixed in this study. This may lead to less calculated errors when using constant parameters to simulate cumulative interception on the basis of a single event. Nonetheless, using short-term parameters may slightly weaken this mutual compensation effect, resulting in a higher error for RSGM-E than for RSGM-M and RSGM-G. Consequently, using fixed climatic parameters in the model calculation, the accuracies of individual intercepted events were also improved (Table 5 and Figure 3), although this improvement was still inadequate to meet the expected requirements. Furthermore, this modeling approach will improve the user-friendliness of the model, because it is less complex, less computationally difficult, and cost-effective. Additionally, it requires tests to be conducted in more areas and includes more tree species, as this study only demonstrated the effectiveness for Pt, Po, and At, while Zhang *et al.* (2018) suggested using storm-based parameters (both canopy and climatic) to run the model in shrub forests.

A previous study demonstrated that the model operates better in storms in which I is strongly dependent on S (canopy structure conditions), whereas meteorological parameters dominate the modeling accuracy when the storms could rapidly saturate the canopy (Sadeghi *et al.* 2015). A study indicated that for the dormant season with lower S-values than the growing season, storms that saturated the canopy occurred more frequently and climatic parameters had a greater influence on interception (Ma *et al.* 2019). In the present study, better model results were obtained using fixed climatic parameters, when the canopy parameters were constant, which is closely similar to the changes in canopy structural conditions during the dormant period. This implies that such use of the model may also lead to a positive result during the dormant period for Pt, Po, and At. However, given the possible differences in rainfall patterns between the dormant and growing seasons in the study area, this is still a speculation that requires further experimentation for verification.

Even though fixed climatic parameters were used in this study, the RSGM performed poorly in estimating individual interception events. The detailed reasons for this have been discussed by Linhoss & Siegert (2020), such as measurement errors and conceptual errors in the model. This result indicates that the modeling canopy interception or even the entire ecohydrological cycle process remains a great challenge, especially for extreme precipitation events (few but intense rainfall events) that are expected to become more frequent in the context of climate change. Hence, increasing the simulation accuracy of the RSGM for a single rainfall event is still a pressing problem.

The sensitivity analysis showed that the cumulative canopy interception is most sensitive to S parameter, whereas climatic parameters (i.e., $\bar{E}_c$ and $\bar{R}$) have lower influence on the estimated interception than S, but generally have greater influence than S_t and p_t, and, at times, have greater influence than c. Similar sensitivity results were reported by Ma *et al.* (2019) and Liu *et al.* (2018) but not by Fan *et al.* (2014) and Su *et al.* (2016). This difference can be attributed to the rainfall patterns. Sadeghi *et al.* (2015) proposed that I was controlled mainly by climatic parameters during large storms but S played a more significant role during small storms. The amount of rainfall recorded in the present study (427.2–497.2 mm) was similar to that reported by Ma *et al.* (2019) and Liu *et al.* (2018). It was significantly less than that (1,492.1 mm during 1 year and 1,574.0 mm during the growing season) reported by Fan *et al.* (2014) and Su *et al.* (2016), respectively. Hence, if extreme events with less small rainfall become more frequent with climate change, particularly in semi-arid regions with scarce rainfall resources, it is necessary to investigate the possibility of enhancing the accuracy of the RSGM in terms of estimating S and reasonably parameterizing the canopy structure. Recent developments in measurement technology have been allowing direct quantification of S (Van Stan *et al.* 2013). Conversely, if the frequency of intense rainfall tends to increase with climate change

(Limousin *et al.* 2008), methods for correctly and conveniently estimating and climatic parameters for forests will assist RSGM modeling. Pereira *et al.* (2016) indicated that the wet-bulb approach was a good alternative for estimating the maximum evaporation rates within very sparse forests with a narrow canopy depth. However, the Penman–Monteith approach seemed preferable when the canopy was not fully ventilated. Given its ability to minimize unnecessary simulation errors due to different methods, the Penman–Monteith approach was uniformly used for forests with different plant densities in the present study. Furthermore, the choice of storm separation time could affect the calculated values of $\bar{R}$ (Wallace & McJannet 2006), thereby influencing the modeled results. To ensure that the canopy remains dry as much as possible as assumed by the model, an interval of 8 h was maintained between all rainfall events during the study period, which is slightly larger than those maintained in previous studies, which were 3 h (Ghimire *et al.* 2017), 4 h (Wallace & McJannet 2008), and 6 h (Ma *et al.* 2019). Wallace & McJannet (2006) reported that uncertainty in the choice of the interval time only impacts the estimated interception by less than 10%.

Although the experimental plots were not far from each other, the presented $\bar{E}_c$ of *Pt* was different from that of the other two species, which can be explained by a malfunction of the data collector, and resulted in several rainfall events that were not monitored by the automatic weather station at *Pt*. Thus, these were directly deleted during the modeling process. Besides, the growing season of a single year was considered in the present study, and to the best of our knowledge, very few studies had reported that the interannual variation in rainfall patterns is small for the study region, whereas the opposite is probably true. The study area has a temperate monsoon climate, and rainfall is mainly influenced by the southeastern monsoon and simultaneous rain and hot climate (Cheng *et al.* 2016). This implies that there is variability in rainfall patterns across years and seasons in the study area, but we speculated that as long as the climate of the study area was characterized by simultaneous rain and hot climate during the study period, the complementary effect between $\bar{R}$ and $\bar{E}_c$ would be maintained and the conclusions of this study could be considered effective. Therefore, it is beneficial to encourage argumentation of these findings in different climate-type regions for the application and development of the model. However, these should not affect the primary goal of the study, which explored the effect of time-step variability in climatic parameters on modeling accuracy, rather than the modeling diversity among different tree species.

5. CONCLUSIONS

This study was conducted to examine the reasonableness of the assumption in the RSGM that the meteorological parameters are the same for all storms, and to explore the differences in the estimation results for single storms when the RSGM was driven by three time-step climate parameters, respectively. The obtained results indicated that all the indicators used to evaluate the model's accuracy were improved if the time step of the climatic parameters ($\bar{R}$ and $\bar{E}_c$) involved in the modeling were increased when the models were run on an event basis, regardless of whether the model was run for *Pt*, *Po*, or *At*. This indicates that the assumption in the RSGM is correct in the study region during the growing season. Fixed climatic parameters were more suitable for predicting cumulative interception in *Pt*, *Po*, and *At* during the growing season in the studied region, whereas meteorological parameters, when averaged for a single event, cannot be usefully applied in the RSGM to obtain satisfying estimations. Nonetheless, the prediction accuracy of the RSGM for individual intercepted events was poor regardless of the time-step variability used. The satisfactory performance obtained using fixed climatic parameters can be associated with a compensation between the overestimation of small rainfall events and the underestimation of large rainfall events. These results indicate that when planning forest restructuring and water resources rational allocation initiatives, it is more appropriate to use fixed climatic parameters to run the RSGM to estimate *I* for *Pt*, *Po*, or *At* in Northern China during the growing season. Further studies are required to confirm this conclusion across the widest possible range of species, regions, and temporal scales to clarify the detailed reasons for this effect. Moreover, future studies could attempt to prove a conjecture that unknown complementary effects between climate parameters on long time scales may have contributed to such better model performance when fixed climate parameters are used, which would lead a better understanding and application of the relevant assumptions in the RSGM.

ACKNOWLEDGEMENTS

This work was funded by a project of the Key Laboratory of Water Saving Irrigation Project of the Ministry of Agriculture (Farmland Irrigation Research Institute of Chinese Academy of Agricultural Sciences, No. FIRI2018-04). We appreciate the constructive comments from the editors and anonymous reviewers that helped to improve the quality of this paper.

DATA AVAILABILITY STATEMENT

Data cannot be made publicly available; readers should contact the corresponding author for details.

REFERENCES

Allen, R. G., Pereira, L. S., Raes, D. & Smith, M. 1998 *Crop Evapotranspiration – Guidelines for Computing Crop Water Requirements*, FAO Irrigation and Drainage Paper No. 56. FAO 300, 6541.

Amiri-Ardakani, Y. & Najafzadeh, M. 2021 Pipe break rate assessment while considering physical and operational factors: a methodology based on global positioning system and data-driven techniques. *Water Resources Management* **35** (11), 3703–3720. doi:10.1007/s11269-021-02911-6.

Attarod, P., Sadeghi, S. M. M., Pypker, T. G., Bagheri, H., Bagheri, M. & Bayramzadeh, V. 2015 Needle-leaved trees impacts on rainfall interception and canopy storage capacity in an arid environment. *New Forests* **46** (3), 339–355. doi:10.1007/s11056-014-9464-2.

Bulcock, H. H. & Jewitt, G. P. W. 2012 Modelling canopy and litter interception in commercial forest plantations in South Africa using the Variable Storage Gash model and idealised drying curves. *Hydrology and Earth System Sciences* **16** (12), 4693–4705. doi:10.5194/hess-16-4693-2012.

Chen, S., Chen, C., Zou, C. B., Stebler, E., Zhang, S., Hou, L. & Wang, D. 2013 Application of Gash analytical model and parameterized Fan model to estimate canopy interception of a Chinese red pine forest. *Journal of Forest Research* **18** (4), 335–344. doi:10.1007/s10310-012-0364-z.

Cheng, T. T., Li, S., Zhang, X. G. & Zhang, Y. T. 2016 Study on the relationship between rainfall and runoff in Yaoxiang small watershed of Shandong province. *Journal of Soil and Water Conservation* **30** (02), 34–37. doi:10.13870/j.cnki.stbcxb.2016.02.006.

Deguchi, A., Hattori, S. & Park, H. 2006 The influence of seasonal changes in canopy structure on interception loss: application of the revised Gash model. *Journal of Hydrology* **318** (1–4), 80–102. doi:10.1016/j.jhydrol.2005.06.005.

Fan, J., Oestergaard, K. T., Guyot, A. & Lockington, D. A. 2014 Measuring and modeling rainfall interception losses by a native Banksia woodland and an exotic pine plantation in subtropical coastal Australia. *Journal of Hydrology* **515**, 156–165. doi:10.1016/j.jhydrol.2014.04.066.

Fathizadeh, O., Hosseini, S. M., Zimmermann, A., Keim, R. F. & Darvishi Boloorani, A. 2017 Estimating linkages between forest structural variables and rainfall interception parameters in semi-arid deciduous oak forest stands. *Science of the Total Environment* **601–602**, 1824–1837. doi:10.1016/j.scitotenv.2017.05.233.

Fathizadeh, O., Hosseini, S. M., Keim, R. F. & Boloorani, A. D. 2018 A seasonal evaluation of the reformulated Gash interception model for semi-arid deciduous oak forest stands. *Forest Ecology and Management* **409**, 601–613. doi:10.1016/j.foreco.2017.11.058.

Gash, J. H. C. 1979 An analytical model of rainfall interception by forests. *Quarterly Journal of the Royal Meteorological Society* **105**, 43–55. doi:10.1002/qj.49710544304.

Gash, J. H. C., Lloyd, C. R. & Lachaud, G. 1995 Estimating sparse forest rainfall interception with an analytical model. *Journal of Hydrology* **170** (1), 79–86. doi:10.1016/0022-1694(95)02697-N.

Ghimire, C. P., Bruijnzeel, L. A., Lubczynski, M. W. & Bonell, M. 2012 Rainfall interception by natural and planted forests in the Middle Mountains of Central Nepal. *Journal of Hydrology* **475**, 270–280. doi:10.1016/j.jhydrol.2012.09.051.

Ghimire, C. P., Bruijnzeel, L. A., Lubczynski, M. W., Ravelona, M., Zwartendijk, B. W. & van Meerveld, H. J. I. 2017 Measurement and modeling of rainfall interception by two differently aged secondary forests in upland eastern Madagascar. *Journal of Hydrology* **545**, 212–225. doi:10.1016/j.jhydrol.2016.10.032.

Hanchi, A. & Rapp, M. 1997 Stemflow determination in forest stands. *Forest Ecology and Management* **97** (3), 231–235. doi:10.1016/S0378-1127(97)00066-2.

Hassan, S. M. T., Ghimire, C. P. & Lubczynski, M. W. 2017 Remote sensing upscaling of interception loss from isolated oaks: Sardon catchment case study, Spain. *Journal of Hydrology* **555**, 489–505. doi:10.1016/j.jhydrol.2017.08.016.

Iida, S., Tanaka, T. & Sugita, M. 2005 Change of interception process due to the succession from Japanese red pine to evergreen oak. *Journal of Hydrology* **315** (1–4), 154–166. doi:10.1016/j.jhydrol.2005.03.024.

Jackson, N. A. 2000 Measured and modelled rainfall interception loss from an agroforestry system in Kenya. *Agricultural and Forest Meteorology* **100** (4), 323–336. https://doi.org/10.1016/S0168-1923(99)00145-8.

Ji, Y. & Cai, T. J. 2015 Canopy interception in original Korean pine forest: measurement and dividual simulation in Xiaoxing'an Mountains, northeastern China. *Journal of Beijing Forestry University* **37** (10), 41–49. doi:10.13332/j.1000-1522.20150084.

Klaassen, W., Bosveld, F. & Water, E. D. 1998 Water storage and evaporation as constituents of rainfall interception. *Journal of Hydrology* **212** (1–4), 36–50. doi:10.1016/S0022-1694(98)00200-5.

Krause, P., Boyle, D. P. & Bäse, F. 2005 Comparison of different efficiency criteria for hydrological model assessment. *Advances in Geosciences* **5** (5), 89–97. doi:10.5194/adgeo-5-89-2005.

Leyton, L., Reynolds, E. R. C. & Thompson, F. B. 1967 Rainfall interception in forest and moorland. In: *International Symposium on Forest Hydrology* (Sopper, W. E. & Lull, H. W., eds). Pergamon, Oxford, pp. 163–178.

Li, Y. M. & Ye, Q. 2019 Climate classification over China based on Köppen climate classification in the context of ENSO. *Climate Change Research* **15** (4), 352–362. doi:10.12006/j.issn.1673-1719.2018.177.

Li, Y., Liu, X., Zhang, C., Li, Z., Zhao, Y. & Niu, Y. 2020 Effect of initial plant density on modeling accuracy of the revised sparse Gash model: a case study of *Pinus tabuliformis* plantations in northern China. *Hydrology Research* **51** (5), 1170–1183. doi:10.2166/nh.2020.007.

Limousin, J., Rambal, S., Ourcival, J. & Joffre, R. 2008 Modelling rainfall interception in a mediterranean *Quercus ilex* ecosystem: lesson from a throughfall exclusion experiment. *Journal of Hydrology* **357** (1–2), 57–66. doi:10.1016/j.jhydrol.2008.05.001.

Linhoss, A. C. & Siegert, C. M. 2016 A comparison of five forest interception models using global sensitivity and uncertainty analysis. *Journal of Hydrology* **538**, 109–116. doi:10.1016/j.jhydrol.2016.04.011.

Linhoss, A. C. & Siegert, C. M. 2020 Calibration reveals limitations in modeling rainfall interception at the storm scale. *Journal of Hydrology* 124624. doi:10.1016/j.jhydrol.2020.124624.

Liu, S., Gao, P., Li, X., Niu, X. & Wang, B. 2015 Canopy rainfall interception characteristics of Chinese fir forest and its revise Gash model simulation in Dagangshan Mountain of Jiangxi province. *Journal of Soil and Water Conservation* **29** (02), 172–176. doi:10.13870/j.cnki.stbcxb.2015.02.032.

Liu, Z., Wang, Y., Tian, A., Liu, Y., Webb, A. A., Wang, Y., Zuo, H., Yu, P., Xiong, W. & Xu, L. 2018 Characteristics of canopy interception and its simulation with a revised Gash model for a larch plantation in the Liupan Mountains, China. *Journal of Forestry Research* **29** (1), 187–198. doi:10.1007/s11676-017-0407-6.

Llorens, P. & Gallart, F. 2000 A simplified method for forest water storage capacity measurement. *Journal of Hydrology* **240** (1–2), 131–144. doi:10.1016/s0022-1694(00)00339-5.

Llorens, P., Domingo, F., Garcia-Estringana, P., Muzylo, A. & Gallart, F. 2014 Canopy wetness patterns in a Mediterranean deciduous stand. *Journal of Hydrology* **512**, 254–262. doi:10.1016/j.jhydrol.2014.03.007.

Lopes, D. D. C., Steidle Neto, A. J., Queiroz, M. G. D., Souza, L. S. B. D., Zolnier, S. & Silva, T. G. F. D. 2020 Sparse Gash model applied to seasonal dry tropical forest. *Journal of Hydrology* **590**, 125497. doi:10.1016/j.jhydrol.2020.125497.

Ma, C., Li, X., Luo, Y., Shao, M. & Jia, X. 2019 The modelling of rainfall interception in growing and dormant seasons for a pine plantation and a black locust plantation in semi-arid Northwest China. *Journal of Hydrology* **577**, 123849. doi:10.1016/j.jhydrol.2019.06.021.

Ma, C., Luo, Y. & Shao, M. 2020 Comparative modeling of the effect of thinning on canopy interception loss in a semiarid black locust (*Robinia pseudoacacia*) plantation in Northwest China. *Journal of Hydrology* **590**, 125234. doi:10.1016/j.jhydrol.2020.125234.

Miralles, D. G., Gash, J. H., Holmes, T. R. H., de Jeu, R. A. M. & Dolman, A. J. 2010 Global canopy interception from satellite observations. *Journal of Geophysical Research* **115**, D16122. doi:10.1029/2009JD013530.

Muzylo, A., Llorens, P., Valente, F., Keizer, J. J., Domingo, F. & Gash, J. H. C. 2009 A review of rainfall interception modelling. *Journal of Hydrology* **370** (1–4), 191–206. doi:10.1016/j.jhydrol.2009.02.058.

Mużyło, A., Valente, F., Domingo, F. & Llorens, P. 2012 Modelling rainfall partitioning with sparse Gash and Rutter models in a downy oak stand in leafed and leafless periods. *Hydrological Processes* **26** (21), 3161–3173. doi:10.1002/hyp.8401.

Najafzadeh, M., Homaei, F. & Farhadi, H. 2021 Reliability assessment of water quality index based on guidelines of national sanitation foundation in natural streams: integration of remote sensing and data-driven models. *Artificial Intelligence Review* **54** (6), 4619–4651. doi:10.1007/s10462-021-10007-1.

Návar, J. 2013 The performance of the reformulated Gash's interception loss model in Mexico's northeastern temperate forests. *Hydrological Processes* **27** (11), 1626–1633. doi:10.1002/hyp.9309.

Pereira, F. L., Valente, F., David, J. S., Jackson, N., Minunno, F. & Gash, J. H. 2016 Rainfall interception modelling: is the wet bulb approach adequate to estimate mean evaporation rate from wet/saturated canopies in all forest types? *Journal of Hydrology* **534**, 606–615. doi:10.1016/j.jhydrol.2016.01.035.

Price, A. G. & Carlyle-Moses, D. E. 2003 Measurement and modelling of growing-season canopy water fluxes in a mature mixed deciduous forest stand, southern Ontario, Canada. *Agricultural and Forest Meteorology* **119** (1), 69–85. doi:10.1016/S0168-1923(03)00117-5.

Ringgaard, R., Herbst, M. & Friborg, T. 2014 Partitioning forest evapotranspiration: interception evaporation and the impact of canopy structure, local and regional advection. *Journal of Hydrology* **517**, 677–690. doi:10.1016/j.jhydrol.2014.06.007.

Rutter, A. J., Kershaw, K. A., Robins, P. C. & Morton, A. J. 1971 A predictive model of rainfall interception in forests, 1. Derivation of the model from observations in a plantation of Corsican pine. *Agricultural Meteorology* **9**, 367–384. doi:10.1016/0002-1571(71)90034-3.

Sadeghi, S. M. M., Attarod, P., Van Stan, J. T., Pypker, T. G. & Dunkerley, D. 2015 Efficiency of the reformulated Gash's interception model in semiarid afforestations. *Agricultural and Forest Meteorology* **201**, 76–85. doi:10.1016/j.agrformet.2014.10.006.

Sheng, H. C., Cai, T. J., Li, Y. & Liu, Y. J. 2014 Rainfall redistribution in *Larix gmelinii* forest on northern of Daxing'an mountains, north-east of China. *Journal of Soil and Water Conservation* **28** (06), 101–105. doi:10.13870/j.cnki.stbcxb.2014.06.019.

Shi, W. & Wang, N. 2020 Improved SMA-based SCS-CN method incorporating storm duration for runoff prediction on the Loess Plateau, China. *Hydrology Research* **51** (3), 443–455. doi:10.2166/nh.2020.140.

Shinohara, Y., Levia, D. F., Komatsu, H., Nogata, M. & Otsuki, K. 2015 Comparative modeling of the effects of intensive thinning on canopy interception loss in a Japanese cedar (*Cryptomeria japonica* D. Don) forest of western Japan. *Agricultural and Forest Meteorology* **214–215**, 148–156. doi:10.1016/j.agrformet.2015.08.257.

Su, L., Zhao, C., Xu, W. & Xie, Z. 2016 Modelling interception loss using the revised Gash model: a case study in a mixed evergreen and deciduous broadleaved forest in China. *Ecohydrology* **9** (8), 1580–1589. doi:10.1002/eco.1749.

Sun, X., Onda, Y. & Kato, H. 2014 Incident rainfall partitioning and canopy interception modeling for an abandoned Japanese cypress stand. *Journal of Forest Research* **19** (3), 317–328. doi:10.1007/s10310-013-0421-2.

Sun, J., Gao, P., Li, C., Wang, R., Niu, X. & Wang, B. 2019 Ecological stoichiometry characteristics of the leaf–litter–soil continuum of *Quercus acutissima* Carr. and *Pinus densiflora* Sieb. in Northern China. *Environmental Earth Sciences* **78** (1). doi:10.1007/s12665-018-8012-3.

Valente, F., David, J. S. & Gash, J. H. C. 1997 Modelling interception loss for two sparse eucalypt and pine forests in central Portugal using reformulated Rutter and Gash analytical models. *Journal of Hydrology* **190** (1), 141–162. doi:10.1016/S0022-1694(96)03066-1.

Valente, F., Gash, J. H., Nóbrega, C., David, J. S. & Pereira, F. L. 2020 Modelling rainfall interception by an olive-grove/pasture system with a sparse tree canopy. *Journal of Hydrology* **581**, 124417. doi:10.1016/j.jhydrol.2019.124417.

van Dijk, A. I. J. M. & Bruijnzeel, L. A. 2001a Modelling rainfall interception by vegetation of variable density using an adapted analytical model. Part 1. Model description. *Journal of Hydrology* **247** (3), 230–238. doi:10.1016/S0022-1694(01)00392-4.

van Dijk, A. I. J. M. & Bruijnzeel, L. A. 2001b Modelling rainfall interception by vegetation of variable density using an adapted analytical model. Part 2. Model validation for a tropical upland mixed cropping system. *Journal of Hydrology* **247** (3), 239–262. doi:10.1016/S0022-1694(01)00393-6.

Van Stan, J. T., Martin, K., Friesen, J., Jarvis, M. T., Lundquist, J. D. & Levia, D. F. 2013 Evaluation of an instrumental method to reduce error in canopy water storage estimates via mechanical displacement. *Water Resources Research* **49** (1), 54–63. doi:10.1029/2012WR012666.

Wallace, J. & McJannet, D. 2006 On interception modelling of a lowland coastal rainforest in northern Queensland, Australia. *Journal of Hydrology* **329** (3), 477–488. doi:10.1016/j.jhydrol.2006.03.003.

Wallace, J. & McJannet, D. 2008 Modelling interception in coastal and montane rainforests in northern Queensland, Australia. *Journal of Hydrology* **348** (3–4), 480–495. doi:10.1016/j.jhydrol.2007.10.019.

Zhang, S., Li, X., Jiang, Z., Li, D. & Lin, H. 2018 Modelling of rainfall partitioning by a deciduous shrub using a variable parameters Gash model. *Ecohydrology* **11** (7), e2011. doi:10.1002/eco.2011.

Zhao, Y., Wang, Y., Wang, Y., Liu, N., Wu, Y. & Chen, L. 2011 Simulation of canopy rainfall interception of the *Phyllostachys edulis* forest with the revised Gash model in the Jinyun Mountains of Chongqing. *Scientia Silvae Sinicae* **47** (09), 15–20.

Zhu, G. R. & Li, Y. 2015 Types and changes of Chinese climate zones from 1961 to 2013 based on Köppen climate classification. *Arid Land Geography* **38** (06), 1121–1132.

First received 3 August 2021; accepted in revised form 21 October 2021. Available online 2 November 2021